Rotational dynamics of type I Fc_ϵ receptors on individually-selected rat mast cells studied by polarized fluorescence depletion

N. A. Rahman,* I. Pecht,‡ D. A. Roess,§ and B. G. Barisas*
*Departments of Chemistry and §Physiology, Colorado State University, Fort Collins, CO 80523 USA; and ‡Department of Chemical Immunology, Weizmann Institute of Science, Rehovoth, Israel

ABSTRACT We report the first application of polarized fluorescence depletion (PFD), a technique which combines the sensitivity of fluorescence detection with the long lifetimes of triplet probes, to the measurement of membrane protein rotational diffusion on individually selected, intact mammalian cells. We have examined the rotation of type I Fc_ϵ receptors ($Fc_\epsilon RI$) on rat mucosal mast cells of the RBL-2H3 line in their resting monomeric and differently oligomerized states using as probes IgE and three monoclonal antibodies (mAbs; H10, J17, and F4) specific for the $Fc_\epsilon RI$. PFD experiments using eosin (EITC)-IgE show that individual $Fc_\epsilon RI$ on cells have a rotational correlation time (RCT) at 4°C of 79 ± 4 μs. Similarly, $Fc_\epsilon RI$-bound EITC-Fab fragments of the J17 $Fc_\epsilon RI$-specific mAb exhibit an RCT of 76 ± 6 μs. These values agree with previous measurements of $Fc_\epsilon RI$-bound IgE rotation by time-resolved phosphorescence anisotropy methods. Receptor-bound EITC-conjugated divalent J17 antibody exhibits an increased RCT of 140 ± 6 μs. This is consistent with the ability of this mAb to form substantial amounts of $Fc_\epsilon RI$ dimers on these cell surfaces. The ratio of limiting to initial anisotropy in these experiments remains constant at about 0.5 from 5°C through 25°C for IgE, Fab, and intact mAb receptor ligands. Extensive cross-linking by second antibody of cell-bound IgE, of intact $Fc_\epsilon RI$-specific mAbs or of their Fab fragments, however, produced large fixed anisotropies demonstrating, under these conditions, receptor immobilization in large aggregates. PFD using the mAbs H10 and F4 as receptor probes yielded values for triplet lifetimes, RCT values, and anisotropy parameters essentially indistinguishable from those obtained with the mAb J17 clone. Possible explanations for these observations are discussed.

INTRODUCTION

In this study we demonstrate the capability of a novel technique employing triplet-state probes, polarized fluorescence depletion (PFD), for measuring membrane protein rotational diffusion. This method, initially introduced by Johnson and Garland (1981, 1982), combines the high sensitivity of fluorescence detection with the long lifetimes of molecular triplet states to measure rotational correlation times in the 10-μs to 1-ms range. The technique has previously been applied to protein rotation on erythrocyte ghosts (Garland and Johnson, 1985) and to suspensions of A431 cells (Corin et al., 1987). We have extended its application to the study of protein rotation on individually-selected, intact mammalian cells. Unlike time-resolved phosphorescence anisotropy methods which require 10^5–10^6 cells per measurement, PFD can be performed in a microscope-based system in which cells are individually selected and then examined.

Measurements of membrane protein dynamics are of considerable interest because the rates of both lateral and rotational movement in the plasma membrane reflect the sizes of proteins involved. Fluorescence photobleaching recovery (FPR) and electromigration techniques enable lateral diffusion of isolated and aggregated membrane receptors to be measured (Schlessinger et al., 1976; McCloskey et al., 1984). Unfortunately, translational diffusion reflects protein motion over macroscopic distances of one micrometer or more and there is only a weak (logarithmic) dependence on molecular weight (Saffman and Delbrück, 1975). On the other hand, rotational correlation times depend linearly on molecular weight and, moreover, reflect the immediate environment of an individual molecule or of a molecular assembly (Chapman and Restall, 1979). Changes in rotational motions of membrane proteins in response to ligand binding thus indicate protein aggregation or oligomerization (Damjanovich et al., 1983; Zidovetzki et al., 1985, 1986).

The Type I Fc_ϵ receptor ($Fc_\epsilon RI$) is a particularly interesting system where ligand-induced molecular aggregation can be investigated. It is generally agreed that mast cell and basophil degranulation are initiated by transmembrane signals generated when cell surface $Fc_\epsilon RI$ are crosslinked. It is clear that only a relatively small fraction of $Fc_\epsilon RI$ need be so aggregated to induce degranulation (Ortega et al., 1988); however, the minimum number of receptors that must be aggregated to generate a unit signal for degranulation is less certain. Early studies on rat serosal mast cells using chemically crosslinked IgE indicated that forming dimers of the Fc_ϵ

0006-3495/91/02/334/13 $2.00

receptors is sufficient to stimulate degranulation (Segal et al., 1977). Similar studies on human basophils (Sobotka et al., 1981) and on rat mucosal mast cells (RBL line) (Fewtrell and Metzger, 1980) using chemically crosslinked oligomers of IgE suggested that cells were more responsive to receptor trimers or oligomers. Studies by Balakrishnan et al. (1982) suggest that clustering and not crosslinking of these $Fc_\epsilon RI$ can cause degranulation. More recently, Baird and coworkers (1988) have extensively examined physicochemical aspects of IgE-mediated cellular degranulation such as effects of the length of cross-linking ligands.

In previous investigations of the role of receptor aggregation in basophils and mast cells, a recurrent problem has been the difficulties in producing homogeneously sized receptor aggregates on the cell surface. Also, in studies where covalent IgE oligomers were fractionated by size, they were cross-linked at unknown loci, hence producing structures of indeterminate topology and conformation (Fewtrell and Metzger, 1980). This makes it difficult to determine how effective are aggregates of a particular size in generating initial secretion inducing signals. It has been argued that high extents of receptor oligomerization may be more effective in cell stimulation only because they also induce markedly enhanced numbers of receptor dimers (Fewtrell and Metzger, 1980; Erikson et al., 1986). We therefore employed a panel of monoclonal antibodies against the $Fc_\epsilon RI$ on rat mucosal mast cells (RBL). Studies using these IgG class monoclonal antibodies (mAbs) demonstrate that they bind to $Fc_\epsilon RI$ on living cell surfaces forming substantial, though different, amounts of receptor dimers. Moreover, because these three different mAbs probably recognize their respective epitopes in distinct ways, they would be expected to yield differently structured $Fc_\epsilon RI$ dimers (Ortega et al., 1989). Using PFD methods it is possible to evaluate rotational motions of $Fc_\epsilon RI$ following binding to these ligands, their Fab fragments, and IgE.

MATERIALS AND METHODS

Chemicals and antibodies

High glucose Dulbecco's Modified Essential Medium (DMEM) was purchased from Hazelton Biologics (Lenexa, KS). Medium was supplemented with fetal calf serum (Irvine Scientific, Irvine, CA), L-glutamine and penicillin-streptomycin (KC Biologics, Lenexa, KS). Eosin isothiocyanate (EITC) was obtained from Molecular Probes (Eugene, OR). D-Glucose, trypsin-EDTA and the enzymes glucose oxidase and catalase were purchased from Sigma Chemical Company (St. Louis, MO). A monoclonal murine IgE specific for DNP haptens and binding with high affinity to the 2H3 $Fc_\epsilon R$ was prepared according to the method of Liu et al. (1980). The preparation and isolation of the F4, H10 and J17 mAbs have been described elsewhere (Ortega et al., 1988). Rat anti-mouse IgG_1 and IgG_2 were obtained from American Qualex (Los Angeles, CA), and mouse anti-rat IgE was purchased from Accurate Chemical Company (Newark, NJ).

The method for labeling antibodies with fluorescent probes was a modification of a previously published technique (Jovin et al., 1981). Antibodies were suspended in phosphate buffered saline (PBS) solution containing 50 mM sodium borate, pH 9.2. The concentration of antibody in solution was determined spectrophotometrically at 280 nm assuming $\epsilon^{1\%}_{280} = 14.7\ cm^{-1}$. 10 mg of eosin isothiocyanate (EITC) was dissolved in 50 μl DMSO and diluted with 50 mM sodium borate solution (pH 9.2). Conjugation of the EITC solution was determined spectrophotometrically at 522 nm assuming $\epsilon^{M}_{522} = 83{,}000$. To ensure at least a 1:1 molar conjugation of dye to antibody, an approximately three-fold molar excess of EITC to antibody was added to the antibody solution. The reaction mixture was incubated overnight at 4°C under subdued light. At the end of the incubation period, the reaction was quenched by adjusting the reaction mixture pH to 7.0 with 1M Tris HCl solution.

To remove unconjugated dye, the mixture was passed through a G25-150 Sephadex column equilibrated with PBS. Column flow rate was 30 ml/cm^2 h for a 1.5-cm diameter column. Free dye and its hydrolysis products were removed by three extractions with one volume of *n*-butanol. Gentle agitation effectively removed free dye without causing substantial protein degradation (Roess et al., 1987). Dissolved butanol was removed by dialysis against PBS. Numbers of EITC per protein molecule and the concentration of protein in solution were determined spectrophotometrically. For ϵ-N-EITC-L-lysine in solution, ϵ^{M}_{280} was determined to be 21,600 cm^{-1} and this value was used to correct for the absorbance contribution of EITC at 280 nm. Typically the degree of conjugation was 1 to 2 mol of EITC per mol of antibody. Antibody preparation were centrifuged at 130,000 *g* for 5 min in a Beckman Airfuge (Beckman Instruments Inc., Palo Alto, CA) before use to remove protein aggregates which form during storage.

Cell culture and labeling

2H3 cells are a subclone of the rat basophil leukemia (RBL) cell line (Barsumian et al., 1981). These cells were a generous gift of Dr. Donna Arndt-Jovin of the Max Planck Institute for Biophysical Chemistry, Goettingen, Germany. Cells were maintained in continuous culture and harvested using methods previously described (Zidovetzki et al., 1986). Harvested cells were washed twice and resuspended in chilled balanced salt solution (BSS) before labeling. Typically, 10^6 to 10^7 cells were labeled per experiment. Cells were then incubated with EITC-derivatized antibodies. In experiments where the surface receptors on cells were secondarily crosslinked with anti-IgE or anti-IgG, cells were incubated in 0.1% NaN_3 (w/v) in BSS at 37°C for 1 h before labeling to prevent endocytosis of the antibodies on the cell surface.

The optimum concentration of antibodies to be used for labeling were determined by incubating samples of 10^6 cells with increasing concentrations of EITC-derivatized antibodies in a total vol of 1 ml of 1 mg/ml BSA in BSS (BSA, Sigma Chemical Co., St. Louis, MO). Fluorescence from labeled cells was measured and plotted versus the amount of EITC-Ab added. Specificity of binding of the labeled antibody was also determined. Cell receptors were first saturated by incubating the cells with a three- to four-fold molar excess of unlabeled antibody. After incubation, cells were pelleted and incubated with optimum amounts of labeled antibodies in BSS containing 1 mg/ml BSA for 1 h at 4°C. Cells were interrogated under a Zeiss Universal fluorescence microscope and the fluorescence per cell was measured. Specific binding of labeled antibodies was indicated when fluorescence of preincubated cells was < 10% of that observed for unblocked cells.

If unlabeled antibody failed to block fluorescence resulting from treatment with EITC-conjugated antibody, butanol extraction of the EITC-derivatized Ab solution was repeated until specific binding was obtained.

Preparation of cells for polarized fluorescence depletion measurements

After labeling cells were washed two to three times by centrifugation at 300 *g* for 10 min in BSS to remove any unconjugated antibody. Pelleted cells were resuspended in deaerated 4-2-(hydroxyethyl)-1-piperazineethanesulfonic acid (HEPES) buffered BSS. To deoxygenate the cells, 50 mM D-glucose, 0.2 mg/ml glucose oxidase (Sigma type II-S) and 0.25 mg/ml catalase (Sigma type C-10) were added to the cell suspension (Johnson and Garland, 1981). The suspension was incubated in a 37°C water bath for 5 min before the cells were pelleted. The pelleted cells were gently resuspended in 0.5 ml of supernatant and placed on a quartz Suprasil 20 slide (Heraus Amersil, Sayville, NJ). A coverslip was glued in place over the cells with quick-setting epoxy resin and cells were then studied by PFD.

Polarized fluorescence depletion measurements

PFD measurements involve modulation of both the polarization and the intensity of exciting light. A low intensity vertically polarized probe beam initially irradiates a sample to determine its steady-state fluorescence intensity I_0. Next, the sample is exposed to a brief but high intensity pulse of vertically polarized light. This pulse is preferentially absorbed by fluorophores whose absorption transition dipoles are vertically aligned. The resulting conversion of these molecules to the nonfluorescent triplet state anisotropically depletes the ground state. The probe beam is applied again and the time-evolution of fluorescence from ground state molecules is monitored.

Recovery of fluorescence occurs by two mechanisms. The first is decay of the triplet excited state molecules back to the ground state, thus causing fluorescence to increase exponentially with time, the time constant being the triplet state lifetime. The second mechanism of ground state recovery is rotational relaxation of the ground state molecules into the depleted orientation. This also results in an exponential increase of fluorescence intensity with time, the time constant being here the rotational correlation time.

After fluorescence has completely recovered to its predepletion value, a second cycle is initiated with the probe beam horizontally polarized. The recovery of fluorescence intensity following the pulse depends on the same two exponentials as in the first cycle. An exponential increase in intensity is observed from triplet decay. However, because the ground state is depleted of fluorophores whose absorption transition dipoles are vertical, fluorophores with horizontally aligned absorption transition dipoles will rotationally relax into the depleted orientation. Thus, rotational relaxation of molecules during the second cycle results in an exponential decrease of fluorescence intensity with time. Therefore, in the first PFD cycle fluorescence is probed by a beam polarized parallel to the depletion pulse, fluorescence recovery $I_{\parallel}(t)$ proceeds as the sum of two exponentials. In the second cycle, fluorescence is probed by a beam that is perpendicular to the depletion pulse, and fluorescence recovery $I_{\perp}(t)$ is equal to the difference of the same two exponentials. A diagram of the polarized fluorescence depletion (PFD) system in shown in Fig. 1.

The continuous wave argon ion lasers used previously in PFD measurements have insufficient power to adequately deplete the ground state of triplet probes in less than a few μs (Yoshida and Barisas, 1986). This is an unacceptably long time for measurements of membrane protein rotation. Therefore, we employed two lasers for measurements of surface protein rotation on 2H3 cells. The frequency-doubled 532 nm output from a Spectra Physics DCR-11 Nd:YAG laser (Spectra Physics, Albuquerque, NM) constituted the depletion pulses. This laser was operated at 10 Hz with a vertically polarized TEM 01 output of less than 40 mJ. The minimum power affording approximately 30% initial fluorescence depletion was employed. A 3× Galilean telescope reduced the beam diameter to that of the argon ion probe laser. Three 90° reflections of the laser beam off a beam splitter, a mirror and a glass plate, respectively, functioned to attenuate the laser power by 200-fold and also to steer the beam into coaxial alignment with the probe beam.

The probe beam was the 514.5-nm line from a Coherent Radiation Innova 90 argon ion laser (Coherent Inc., Palo Alto, CA). The laser operated with a vertically polarized TEM 00 output of 100 mW. A Lasermetrics 3031 transverse Pockels cell (Lasermetrics Inc., Teaneck, NJ), driven by a special MOSFET driver, rotated the plane of polarization of the argon ion laser beam by 90° in < 200 ns. The beam then entered a Coherent 304d acousto-optic modulator (AOM; Coherent Inc., Modulator Division, Danbury, CT). The first-order diffracted beam was aligned with the optical axis and used as the probe beam. The AOM turned off the probe beam between cycles to allow complete recovery of steady-state fluorescence. To compensate for the intensity differences between the orthogonal polarizations which arose from reflection off mirrors and beam splitters, the light passed through a coverslip set at 53° to the vertical axis. The probe beam was then attenuated by a 2.0 neutral density filter (Newport Research Inc., Fountain Valley, CA) before combining with the depletion beam from the Nd:YAG laser. A hard-wired sequencing computer synchronized the timing of the Pockels cells, AOM, and the firing of the flash lamp of the Nd:YAG laser. After two 90° reflections, the colinear beams entered the lateral port of a Zeiss Universal microscope (Carl Zeiss, Thornwood, NJ) fitted with a III/RS epifluorescence illuminator. A 40× objective of numerical aperture 0.65 was used. Fluorescence from the laser-illuminated cell was isolated. In contrast to FPR measurements, no auxiliary lens was used to focus the laser beam onto the image plane in the illuminator. The focused laser spot at the sample thus had a $1/e^2$ radius of 25 μm. Scattered light was blocked by a Zeiss tetramethylrhodamine filter set with an additional Schott KV 550 filter. Fluorescence emitted from variously sized regions of the sample was isolated with a Zeiss MP03 microscope photometer diaphragm and detected using a thermionically cooled EMI 9816A photomultiplier tube (Thorn EMI Gencom Inc., Plainview, NY). Photon counting was used with count rates not exceeding 10^{-6}/s. The PMT was fitted with two ring defocusing magnets (Products for Research Inc., Danvers, MA) to further reduce the dark current. A gating circuit (GB1001A, Thorn EMI, Gencom Inc.) permitted the PMT to be turned off during the periods of intense fluorescence emitted during the depletion pulses.

The optical components associated with the PFD experiment were mounted on an 18 × 24 in sliding optical table which also supported the pulse generator used in fluorescence photobleaching recovery (FPR) measurements. This table in turn was mounted on a larger 4 × 8 ft Newport Research optical bench (Newport Research Inc., Fountain Valley, CA) on which the lasers and microscope systems were also mounted. By sliding the smaller table into either of the two fixed positions, the optical system used either for the PFD or that for the FPR could be placed in the laser beam path. Changing from one experimental technique to another took only a few minutes, allowing measurements of rotational and translational diffusion to be made under similar conditions.

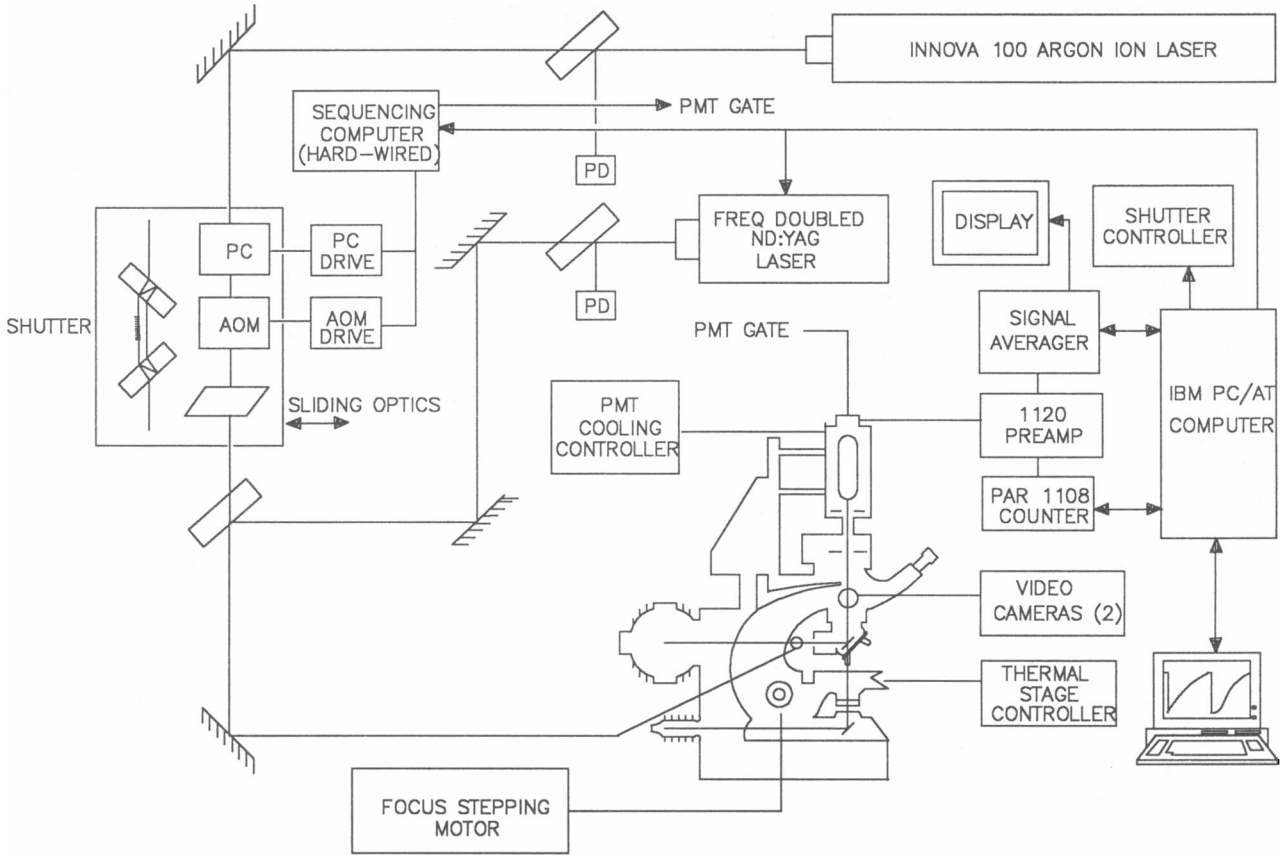

FIGURE 1 Block diagram of microscope-based polarized fluorescence depletion (PFD) system. The frequency-doubled 532 nm output from Nd:YAG laser provides the depletion pulses. The 514.5-nm line from the continuous wave Ar ion laser serves as the probe beam. Data acquired with the Nicolet LAS 12/70 multichannel analyzer are transferred to the IBM PC/AT computer for analysis.

Data analysis

Fluorescence intensities $I_{\parallel}(t)$ and $I_{\perp}(t)$ can be analyzed (Yoshida and Barisas, 1986) to yield a depletion intensity function $s(t)$ and a depletion anisotropy function $r(t)$. These functions are analogous to those obtained from time-resolved phosphorescence anisotropy measurements. We define $s(t)$ and $r(t)$ as follows:

$$s(t) = \Delta I_{\parallel} + 2g\Delta I_{\perp}; \tag{1}$$

where

$$r(t) = \frac{\Delta I_{\parallel} - g\Delta I_{\perp}}{s(t)} \tag{2}$$

$$\Delta I_{\parallel} = I_0 - I_{\parallel}(t); \tag{3}$$

$$\Delta I_{\perp} = I_0 - I_{\perp}(t), \tag{4}$$

and I_0 and g are the predepletion fluorescence and an instrumental constant, respectively. Data collection is halted long enough between cycles to ensure complete recovery of ground state fluorescence so that I_0 values are equal in Eqs. 3 and 4. In our experiments, $s(t)$ was fitted to a multiexponential decay model to obtain the triplet lifetime(s) of the fluorescent probe and the amplitude(s) of their decay. Standard errors in these quantities were assigned by the usual methods (Bevington, 1969). Results from the lifetime analysis were used to weight points in a nonlinear least squares fit of the anisotropy data. Statistical considerations show that the error σ_r in anisotropy is

$$\sigma_r = \frac{2\sqrt{2n}}{s(t)}, \tag{5}$$

where n is the number of counts per channel and $s(t)$ is described in Eq. 1. Using a weighting factor $w_i = 1/\sigma_r^2$ permitted anisotropy decay data to be properly analyzed according to a single exponential decay model.

$$r(t) = r_{\infty} + (r_0 - r_{\infty}) \exp(-t/\phi) \tag{6}$$

Fitting $r(t)$ to Eq. 6 yielded the initial anisotropy value r_0, the limiting anisotropy value r_{∞}, and the rotational correlation time ϕ as well as the statistical uncertainties in these quantities (Bevington, 1969). It should be noted that standard techniques used in nonlinear curve fitting yield uncertainties in such quantities which are usually less than the true uncertainties. However, from our available experimental data, true estimates of these uncertainties cannot be assessed.

RESULTS

Preincubation of 2H3-RBL cells with unlabeled $Fc_\epsilon RI$-specific mAbs reduced by 90% cell fluorescence resulting from subsequent treatment with EITC-labeled mAbs. Thus, fluorescence observed in these studies was due to specific binding of these ligands to the cell surface receptor and not due to nonspecific labeling. We found size exclusion chromatography followed by *n*-butanol extraction to be effective in removing unconjugated EITC from the antibody preparation. It is critical that antibody preparations be free of unconjugated dye which binds nonspecifically to cells yielding decreased overall anisotropy values. In the absence of such careful purification of antibody conjugates, adequate binding specificity could not be obtained.

Measurements of the rotational motion of the $Fc_\epsilon RI$ on 2H3-RBL cells were performed on individual cells or on small clumps of up to five cells. Fluorescence from the cells was isolated using the aperture diaphragm of the Zeiss MP03 microscope photometer. Typically 4096 depletion-recovery cycles were recorded per sample. Because the samples are deoxygenated, the overall amount of irreversible photobleaching is small, $<20\%$ after 4096 depletion-recovery cycles. Because values of $I_\parallel(t)$ and $I_\perp(t)$ are acquired from alternating cycles and compared with each other, the effect of this irreversible photobleaching is negligible. Eq. 5 shows that $\sim 10^5$ counts per channel are required to reduce the uncertainty in initial anisotropy to <0.01. Thus, to enhance signal-to-noise ratio, 30 to 40 samples obtained under identical conditions were summed to a single data set. Fig. 2 shows a typical raw data trace obtained at 4°C from a single 2H3-RBL cell binding EITC-derivatized H10 $Fc_\epsilon RI$-specific monoclonal antibody. The left half of the trace was obtained with the probe beam and depletion pulse polarized parallel to each other. The right half of the trace was obtained, after a 100-ms delay to allow triplet decay and Nd:YAG laser recharge, with the two lasers polarized perpendicular to each other. That a single cell measurement contained substantial information on receptor rotation is apparent from the difference in curvature of the left and right traces in the region immediately following the depletion pulses. Fig. 3 is the summed intensity function for ~ 30 2H3 cells fitted to a two-exponential decay model. We obtained two lifetime values of 76 ± 5 μs and 285 ± 14 μs with relative amplitudes of 0.45 and 0.55, respectively.

Fig. 4 shows plots of anisotropy decay for rotation of $Fc_\epsilon RI$ in various aggregation states at 4°C. Nonlinear least squares analysis of the anistropy data indicated that Eq. 5 satisfactorily represents anisotropy decay as a single exponential decay leading to a finite limiting anisotropy value.

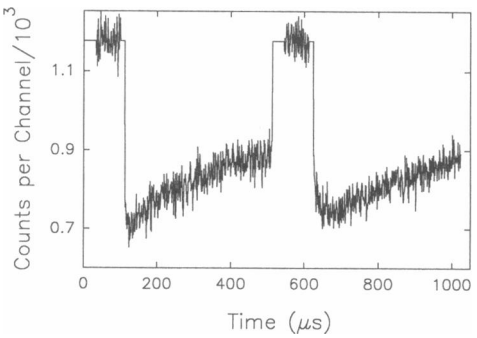

FIGURE 2 Raw PFD data for rotation of $Fc_\epsilon RI$ on a single 2H3-RBL cell at 4°C. EITC-derivatized H10 $Fc_\epsilon RI$-specific monoclonal antibodies were used as the receptor ligands. Approximately 0.3 pmols of these mAbs were required to saturate 0.6 pmols $Fc_\epsilon RI$. Each half of the trace shows recovery of steady-state fluorescence following depletion by the YAG laser pulse. The gating periods are the flat 10-μs sections to the right of the initial fluorescence regions. The exciting pulses occur in the middle of the gating periods. In the left and right halves of the trace, the probe beam was polarized parallel and perpendicular, respectively, to the depletion pulse. That a single cell measurement contains substantial information on receptor rotation is apparent from the difference in curvature of the left and right traces in the region immediately following the depletion pulses.

The goodness of fit could be assessed from the magnitude χ_r^2 of the reduced chi-squared:

$$\chi_r^2 = \left(\sum_{i=1}^{n} w_i[r_{obs}(t) - r_{calc}(t)]^2\right)/(l-3), \qquad (7)$$

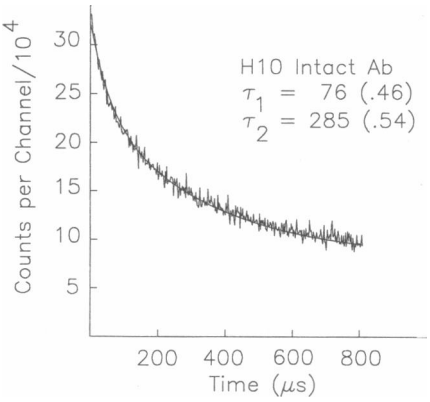

FIGURE 3 Intensity function ($\Delta I_\parallel + 2g\Delta I_\perp$) for a summed data set consisting of 20 traces plotted versus time after exciting light pulse. Each trace was obtained from single to small clumps of cells labeled with EITC-derivatized H10 $Fc_\epsilon RI$-specific monoclonal antibodies at 4°C. When these data were fitted to a two-exponential decay model, triplet lifetime values of 76 and 285 μs with fractional amplitudes of 0.42 and 0.58, respectively, were obtained.

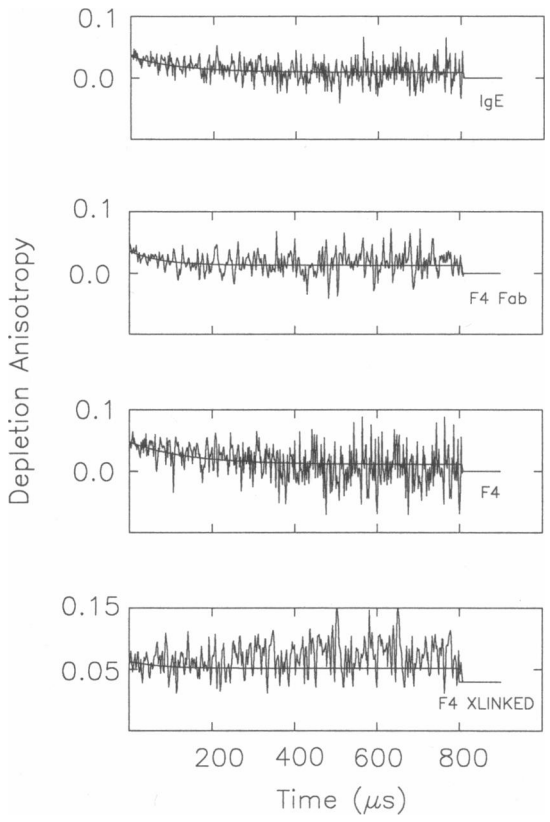

FIGURE 4 Anisotropy decay curves of EITC-labeled $Fc_\epsilon RI$-bound ligands in different aggregation states plotted versus time after exciting light pulse. From top to bottom, the traces represent the following probes and numbers of summed single cell measurements: EITC-IgE, 76 measurements; EITC-F4-Fab, 56 measurements; EITC-F4-mAb, 50 measurements, EITC-F4-Fab cross-linked by anti-IgG_1, 27 measurements. The rotational correlation times observed are: IgE, 79 μs; F4-Fab, 81 μs; F4-mAb, 171 μs; IgG-cross-linked F4-Fab, > 1,000 μs. The smooth curves are anisotropy data fitted to Eq. 6 using weighting obtained from the corresponding intensity function. Measurements were performed at 4°C.

where w_i as calculated from Eq. 5 is the appropriate statistical weighting factor and l is the number of $I_\parallel$ and $I_\perp$ data pairs. Values of χ_r^2, which ranged from 0.69 to 3.9, indicated satisfactory fit of experimental data to a single exponential decay model of Eq. 6.

Results of analyzed intensity functions are summarized in Table 1. Receptor-bound EITC-conjugates of all three intact mAbs, the corresponding Fab fragments, and the IgE required two triplet lifetimes for a satisfactory fit of PFD data. For example, we observed for the EITC-F4 intact mAb at 4°C, two lifetimes of 114 ± 16 μs and 267 ± 17 μs with relative amplitudes of 0.48 and 0.52, respectively. Similarly, we observed triplet lifetimes of 115 ± 9 μs and 283 ± 14 μs for receptors labeled with EITC-Fab fragments of the F4 mAb with relative amplitudes of 0.47 and 0.53, respectively. In contrast, only a single lifetime was necessary to characterize triplet decay of probes bound to extensively cross-linked receptors and this lifetime was markedly longer than anything observed for nonaggregated receptors. Receptors highly crosslinked by treatment with EITC-F4 intact mAb or its Fab fragments followed by incubation with polyclonal anti-IgG exhibited single triplet lifetimes of 980 ± 9 μs and 713 ± 11 μs, respectively.

The rotational dynamics of the cell surface $Fc_\epsilon RI$ bound Fab fragments of the mAbs were compared with those of receptors binding IgE. Fig. 5 illustrates the anisotropy decays for rotation at 4°C of Fab fragments of all three specific mAbs and of IgE. Results are summarized in Table 2. We found that, at a given temperature, for $Fc_\epsilon RI$ binding Fab fragments of $Fc_\epsilon RI$-specific mAbs, no difference can be resolved among the the anisotropy decay patterns when compared to the receptors binding EITC-IgE molecules. For example, we observed rotational correlation times at 4°C of 79 ± 4 μs and 84 ± 7 μs for $Fc_\epsilon RI$ binding IgE molecules and Fab fragments of F4 mAb, respectively. The H10 and J17 mAbs gave comparable results at 4°C.

When EITC-conjugates of intact $Fc_\epsilon RI$-specific mAbs were used as receptor probes, rotational correlation times were approximately twice those observed with either IgE or mAb Fab fragments (Fig. 4). For example, the rotational correlation time at 4°C of $Fc_\epsilon RI$ binding EITC-conjugated intact J17 $Fc_\epsilon RI$-specific mAb was 140 ± 6 μs compared to 76 ± 6 μs and 79 ± 4 μs for receptor-bound EITC-J17 Fab fragments and EITC-IgE, respectively. A comparably increased in RCT for receptor-bound intact mAb over that observed for receptors binding the corresponding Fab fragment was observed for the other $Fc_\epsilon RI$-specific mAb. Initial anisotropies for $Fc_\epsilon RI$ probed with IgE or with anti-$Fc_\epsilon RI$ mAbs or their Fab fragments were not significantly different. These initial anisotropies averaged 0.039 at 4°C while limiting anisotropies average 0.019. Only small differences in the rotational motion of cell surface $Fc_\epsilon RI$ binding for F4, J17 and H10 $Fc_\epsilon RI$-specific mAbs were noted. Rotational dynamics of the cell surface $Fc_\epsilon RI$ binding Fab fragments of all three $Fc_\epsilon RI$-specific mAbs were statistically indistinguishable, as illustrated by the anisotropy decay traces in Fig. 5 and the results in Table 2. A somewhat larger difference was observed for the RCT of receptors bearing intact H10 $Fc_\epsilon RI$-specific antibodies and those labeled with the F4 intact antibodies. Receptors binding intact H10 antibodies exhibited a rotational correlation time of 121 ± 12 μs, whereas those of the intact F4 antibodies had a rotational correlation time of 171 ± 5 μs at 4°C.

The temperature dependence of anisotropy decay for $Fc_\epsilon RI$ binding intact F4 mAbs are shown in Fig. 6. Numerical results of measurements at 4°C, 15°C and

TABLE 1 **Triplet lifetimes of EITC probes labeling type I Fc_ϵ receptors on 2H3-RBL cells**

2H3 Cells binding		Temp	Lifetimes (μs)[c]	
1st reagent	2nd reagent	(°C)	τ_1	τ_2
(monomers)				
EITC-IgE	none	15	88 ± 4 (.47)[a]	228 ± 14 (.53)[a]
		4	124 ± 19 (.42)[a]	334 ± 30 (.58)[a]
EITC-Fc_ϵRI-specific Fab (F4)	none	15	106 ± 10 (.51)[a]	340 ± 8 (.49)[a]
		4	115 ± 9 (.47)[a]	283 ± 14 (.53)[a]
EITC-Fc_ϵRI-specific Fab (H10)	none	4	133 ± 7 (.46)[a]	302 ± 9 (.54)[a]
EITC-Fc_ϵRI-specific Fab (J17)	none	4	127 ± 8 (.42)[a]	315 ± 14 (.54)[a]
(dimer-containing)				
EITC-Fc_ϵRI-specific Ab (F4)	none	27	96 ± 6 (.57)[a]	214 ± 15 (.43)[a]
		15	78 ± 14(.45)[a]	179 ± 9 (.55)[a]
		4	114 ± 16 (.48)[a]	257 ± 12 (.52)[a]
EITC-Fc_ϵRI-specific Ab (H10)	none	4	76 ± 5 (.42)[a]	285 ± 14 (.58)[a]
EITC-Fc_ϵRI-specific Ab (J17)	none	4	97 ± 12 (.57)[a]	268 ± 17 (.43)[a]
(large aggregates)				
EITC-IgE (anti-DNP)	anti-IgE	4	707 ± 12 (1.0)[b]	
EITC-Fc_ϵRI-specific Fab (F4)	anti-IgG_1	4	979 ± 9 (1.0)[b]	
FC_ϵ-specific Fab (F4)	EITC-anti-IgG_1	15	884 ± 14 (1.0)[b]	
		4	713 ± 11 (1.0)[b]	
EITC-Fc_ϵRI-specific Ab (F4)	anti-IgG_1	15	763 ± 8 (1.0)[b]	
		4	813 ± 8 (1.0)[b]	
EITC-Fc_ϵRI-specific Ab (H10)	anti-IgG_2	4	970 ± 12 (1.0)[b]	
EITC-Fc_ϵRI-specific Ab (J17)	anti-IgG_1	4	984 ± 10 (1.0)[b]	

[a]The values in parentheses are the fraction of total fluorescence depletion attributed to each triplet lifetime. Overall depletion observed ranged between 15 and 22%. [b]Triplet decay of EITC bound to crosslinked antibodies could adequately be represented a single exponential. [c]Error bars are ± one estimated standard deviation of fitted parameters as judged by standard techniques used in nonlinear curve fitting (see text).

27°C are summarized in Tables 1 and 2. Table 1 summarizes the triplet lifetime values of the probe whereas in Table 2, the corresponding anisotropy and RCT values obtained are displayed. Rotational diffusion of the Fc_ϵRI was found to increase with temperature. The calculated heat of activation of viscous flow $\Delta H^\ddagger$ was ~5 kcal/mol for Fab fragment-labeled receptors and 3 kcal/mol for receptors binding intact mAb. The difference between $\Delta H^\ddagger$ values observed for Fab fragments and intact mAbs is insignificant due to the statistical error involved in rotational diffusion measurements. On the average, increasing temperature decreased both the initial and final anisotropy values but the ratio of the final to initial anisotropy remained essentially constant at ~0.48.

That extrinsic cross-linking of Fc_ϵRI-bound IgE or Fc_ϵRI-specific mAbs or their Fab fragments directly hindered the rotational diffusion of the Fc_ϵRI was shown when 2H3 cells, the Fc_ϵRI of which bound mAbs, were incubated with polyclonal anti-mouse IgG antibodies (Fig. 4). These polyclonal anti-IgG antibodies cross-linked the heavy chains of the Fc_ϵRI-specific mAb into large aggregates. This virtually eliminated observable rotational diffusion of the Fc_ϵRI: the anisotropy function showed no decay with time. We concluded that the rotational correlation time exceeded the 1,000-μs time scale of our experiment. The numerical data obtained for Fc_ϵRI rotationally immobilized by cross-linking of bound ligands are summarized in Table 1 and 2. Cross-linking of the bound antibodies with anti-immunoglobulin inhibited the rotational motion of Fc_ϵRI in much the same way for all three mAbs. The initial and limiting anisotropies observed for the cross-linked receptors were, as expected, larger than those of receptors bearing the same first ligand but not subsequently cross-linked. For example, cross-linked receptors at 4°C had average r_0 and r_∞ values of 0.057 and 0.049, respectively vs 0.039 and 0.017, respectively, for the noncross-linked proteins. We also noted that the location of the fluorophore protein label is immaterial in these cross-linking experiments: EITC-conjugates of either mAb or anti-IgG produced identical PFD results. Both combinations of reagents drastically reduced ligand rotational diffusion to a value immeasurable on the time scale of the experiment.

DISCUSSION

Some membrane proteins are expressed at quite low levels on a cell surface. For example, only ~3,100 copies of luteinizing hormone receptors are present on ovine

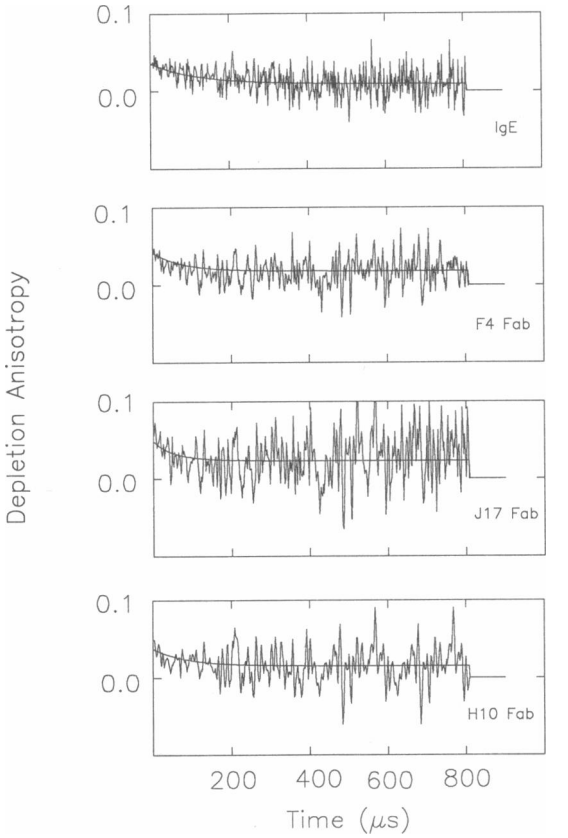

FIGURE 5 Anisotropy decays for rotation at 4°C of 2H3-RBL cell Type I Fc_ϵ receptors binding EITC-Fab fragments of three different $Fc_\epsilon RI$-specific monoclonal antibodies (F4, J17, and H10) and EITC-IgE plotted versus time after exciting light pulse. From top to bottom the traces represent the following $Fc_\epsilon RI$ ligands and numbers of summed single cell measurements: EITC-H10-Fab, 20 measurements; EITC-J17-Fab, 46 measurements; EITC-F4-Fab, 56 measurements; EITC-IgE, 76 measurements. The smooth curves are anisotropy data fitted to Eq. 6 using weighting obtained from the corresponding intensity function.

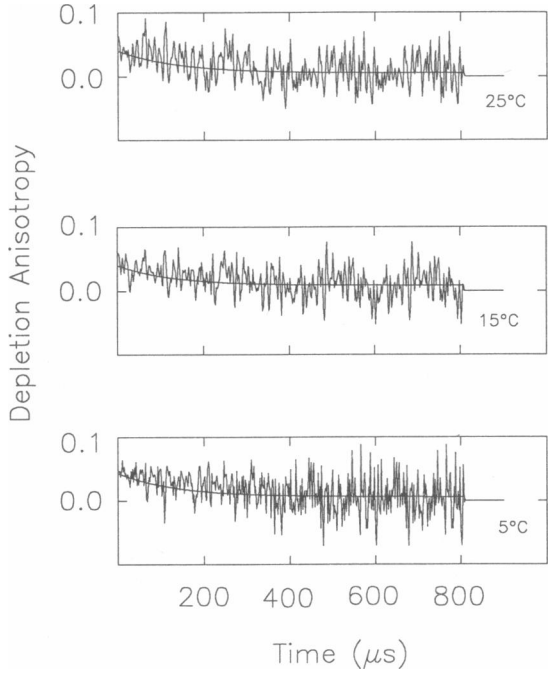

FIGURE 6 Temperature dependence of anisotropy decay kinetics for 2H3-RBL cell Type I Fc_ϵ receptors binding EITC-F4-mAb plotted versus time after exciting light pulse. The rotational correlation times are 171 μs at 4°C, 154 μs at 15°C, and 124 μs at 25°C, a temperature dependence consistent with receptor rotational correlation times being linearly related to plasma membrane lipid bilayer viscosity. The smooth curves are anisotropy data fitted to Eq. 6 using weighting obtained from the corresponding intensity function.

large luteal cells (Niswender et al., 1985) whereas 450,000 to 600,000 copies of $Fc_\epsilon RI$ are present on 2H3 cells (Ortega et al., 1988). These numbers of molecules, together with the rapid microsecond to millisecond timescale of their rotation, mean that only rather sensitive techniques can resolve rotational motions of membrane proteins. Previously, the only technique practical for such measurements has been time-resolved phosphorescence anisotropy, particularly as elaborated by Jovin and collaborators (Aroeti et al. 1990; Jovin and Vaz, 1989; Jovin, 1986; Matayoshi et al, 1991; Matayoshi and Jovin, 1991). Application of this method has, unfortunately, been limited by a number of factors, the most significant of which is the low phosphorescence quantum yield of otherwise-suitable phosphors. Thus, applicability of this method has been restricted to the examination of rather substantial samples in cuvettes, 10^6 to 10^7 cells are prepared per measurement of which perhaps 10^5 to 10^6 cells are actually interrogated optically.

In this study, we demonstrate the capability of another triplet state technique, polarized fluorescence depletion, for measurement of membrane protein rotational diffusion on individually selected, intact cells. PFD combines the inherent sensitivity of fluorescence emission measurements with the long lifetimes of triplet states. PFD requires protein labels with substantial quantum yields both for triplet formation (Φ_t) and for prompt fluorescence (Φ_f). Thus, eosin or 2,4,5,7-tetrabromofluorescein, for which these quantities are comparable ($\Phi_t = 0.7$, $\Phi_f = 0.2$), is very nearly ideal for PFD measurements. At room temperature, the eosin triplet state lifetime is ~2.6 ms (Garland and Moore, 1979) permitting the measurement of rotational correlation times from <10 μs up to 1 ms. Also, because the quantum yield for prompt fluorescence is high, cells binding EITC-derivatized ligands can be visually identified in a fluorescence microscope and the quality of this

TABLE 2 **Rotational diffusion of type I Fc_ϵ Receptors on 2H3-RBL cells**

2H3 Cells Binding		Temperature	anisotropies[b]		RCT[b]
1st reagent	2nd reagent	(°C)	r_0	r_∞	(μs)
(monomers)					
EITC-IgE	none	15	0.048 ± 0.010	0.016 ± 0.014	58 ± 3
		4	0.028 ± 0.011	0.011 ± 0.013	79 ± 4
EITC-Fc_ϵRI-specific Fab (F4)	none	15	0.044 ± 0.010	0.019 ± 0.013	61 ± 4
		4	0.051 ± 0.011	0.030 ± 0.012	84 ± 7
EITC-Fc_ϵRI-specific Fab (H10)	none	4	0.025 ± 0.012	0.012 ± 0.012	83 ± 5
EITC-Fc_ϵRI-specific Fab (J17)	none	4	0.042 ± 0.010	0.020 ± 0.013	76 ± 6
(dimer-containing)					
EITC-Fc_ϵRI-specific Ab (F4)	none	27	0.024 ± 0.011	0.013 ± 0.013	124 ± 5
		15	0.044 ± 0.012	0.021 ± 0.014	154 ± 7
		4	0.048 ± 0.010	0.019 ± 0.011	171 ± 5
EITC-Fc_ϵRI-specific Ab (H10)	none	4	0.036 ± 0.013	0.021 ± 0.016	122 ± 12
EITC-Fc_ϵRI-specific Ab (J17)	none	4	0.044 ± 0.009	0.024 ± 0.022	140 ± 6
(large aggregates)					
EITC-IgE (anti-DNP)	anti-IgE	4	0.041 ± 0.012	0.036 ± 0.014	>1,000[a]
EITC-Fc_ϵRI-specific Fab (F4)	anti-IgG_1	4	0.071 ± 0.012	0.067 ± 0.012	>1,000[a]
EITC-Fc_ϵRI-specific Ab (F4)	anti-IgG_1	15	0.074 ± 0.012	0.064 ± 0.011	>1,000[a]
		4	0.040 ± 0.019	0.031 ± 0.022	>1,000[a]
Fc_ϵRI-specific Fab (F4)	EITC- anti-IgG_1	15	0.071 ± 0.012	0.065 ± 0.013	>1,000[a]
		4	0.043 ± 0.011	0.039 ± 0.014	>1,000[a]
EITC-Fc_ϵRI-specific Ab (H10)	anti-IgG_2	4	0.073 ± 0.011	0.067 ± 0.013	>1,000[a]
EITC-Fc_ϵRI-specific Ab (J17)	anti-IgG_1	4	0.071 ± 0.010	0.063 ± 0.030	>1,000[a]

[a]These quantities exceed the longest rotational correlation time measurable with our system. We estimate this quantity to be ~1,000 μS. [b]Error bars are ± one estimated standard deviation of fitted parameters as judged by standard techniques used in nonlinear curve fitting (see text).

binding assessed. Moreover, EITC-labeled proteins can also be used as probes in fluorescence photobleaching recovery experiments, thus permitting measurements of both the rotational and lateral diffusion of a given cell surface protein to be performed using only a single protein conjugate. Finally, relative to erythrosin or 2,4,5,7-tetraiodofluorescein, which is the chromophore of choice in TPA experiments, EITC-protein conjugates are more easily purified from unreacted dye, far more stable in storage, and less prone to form microparticulates which, if allowed to bind to cell surfaces, give rise to various artifacts in TPA measurements.

The high sensitivity of PFD methods means that significant rotational information can be obtained from observation of a single cell (see Figure 2). Thus a microscope-based PFD optical system, allowing the selection and examination of individual cells, is feasible, whereas analogous single cell measurements are not possible with TPA. In the present studies, for example, each data trace was obtained from individual cells or from small clumps of up to four cells. A composite trace with an acceptable signal-to-noise ratio is obtained from summed 30 to 35 individual traces, i.e., an average of 100–200 cells. Because all cells are microscopically identified and individually selected, PFD methods are suitable for studies of specific cells within heterogeneous cell populations. Moreover, adherent cells can be studied while attached to a substrate.

Using PFD methods, we have examined the rotational diffusion of Fc_ϵRI on 2H3 cells. Triplet states lifetimes calculated from PFD data on nonaggregated receptors binding IgE and Fab fragments of the Fc_ϵRI-specific mAbs are in reasonable agreement with other data on eosin lifetimes. For example, phosphorescence emission studies of cell-bound EITC-concanavalin A (Austin et al., 1979) also showed two lifetime components, 22 μs and 350 μs, with amplitudes of 0.46 and 0.54, respectively, as did fluorescence depletion anisotropy measurement of EITC-concanavalin A on A431 cells where lifetimes of 16 μs and 274 μs with fractional amplitudes of 0.38 and 0.62, respectively, were observed (Corin et al., 1987). Similarly, Fc_ϵRI binding intact mAbs exhibited two triplet state lifetime components. However, only a single, much longer triplet state lifetime is observed for Fc_ϵRI in their aggregated states. Because these longer lifetimes approach the highest values measurable instrumentally, it is not possible to state how many exponential lifetime components might comprise the decay observed. In any case, this much longer mean lifetime could be due to the EITC probe being caged within the cross-linked complex, thus making it inaccessible to triplet quenching by oxygen. However, because

increased lifetimes are also exhibited by EITC conjugated to the second (anti-Ig) antibody, we must admit that we simply do not understand the observation.

Our PFD measurements on $Fc_\epsilon RI$-bound monovalent ligands IgE and Fab fragments of $Fc_\epsilon RI$-specific mAbs yielded rotational parameters consistent with monomeric protein receptors freely rotating about their membrane portion. Values obtained via PFD agree well with those reported using time-resolved phosphorescence anisotropy (Zidovetzki et al., 1986). Zidovetzki and co-workers measured via TPA the rotational correlation time of $Fc_\epsilon RI$ binding rat IgE and reported an average rotational correlation time for the receptor-IgE complex of 65 μs at 5.5°C (1986). A two-exponential analysis of TPA data for receptor-bound IgE rotation implies a mean RCT of 82 μs at 5°C (Pecht et al., 1991; vide infra). These values are comparable with those we obtained for receptor monomers at 4°C. These relatively fast rotational correlation times appear to exclude strong receptor association with the cytoskeleton or with other membrane proteins. This observation is consistent with the lateral mobility of IgE-binding monomeric $Fc_\epsilon RI$. Schlessinger et al. (1976) reported a lateral diffusion coefficient of 3×10^{-10} cm^2 and 85% mobility for these receptors. These values are typical for cell membrane proteins that are not anchored to the underlying cytoskeleton; moreover, studies by Robertson et al. (1986) suggest that interaction of $Fc_\epsilon RI$ with the cytoskeleton only occurs following oligomerization of these receptors. The rotational correlation time of 78–82 μs at 4°C for the receptor-IgE complex is also comparable to those obtained for other integral membrane proteins such as EGF (Zidovetzki et al., 1985).

Our results for the rotational diffusion of the $Fc_\epsilon RI$ bound Fab fragments derived from the different mAbs were comparable to one another and with the receptor-IgE complex. However, low temperature TPA measurements of these Fab-receptor complexes yielded RCTs of 199 μs (H10), 63 μs (J17) and 189 μs (F4), which obviously exhibit considerably more variation. At temperatures near 37°C the same measurements converge to values of ~30 μs which are more consistent with IgE and our data. The authors of this TPA study (Pecht et al., 1991) attribute these differences in rotational dynamics to specific attachment of the probe, erythrosin isothiocyanate, to specific protein sites yielding specific chromophore orientations. The uniformity of our results suggest a more random and less specific labeling of the Fab fragments by our eosin probe.

$Fc_\epsilon RI$-bound specific mAbs exhibited rotational correlation times approximately double that of the IgE binding $Fc_\epsilon RI$ monomers (Zidovetzki et al., 1986). Our rotational diffusion data thus might be taken to suggest that all three mAbs are involved in rotating structures about twice the size of the receptor monomer. However, previous studies suggested that mAbs F4, J17 and H10 formed maximally 20%, 60%, and 100% $Fc_\epsilon RI$ dimers, respectively, on the 2H3 cell surfaces examined (Ortega et al. 1989), the intrinsic receptor binding constants at 25°C being 1×10^7 M^{-1}, 2×10^7 M^{-1}, and 2×10^8 M^{-1} for the F4, J17, and H10 mAbs, respectively. The secretory dose-response of 2H3 cells to these mAbs are also different. F4 mAbs cause secretion of almost 80% of granular content whereas J17 and H10 only induced release of 30% to 40% mediator content. Given the expected differences in the extents of dimer formation, the increased RCTs of intact mAbs relative to Fab fragments must arise not only from receptor dimer formation but also from structural differences in the dimeric species formed (Ortega et al., 1988). Recruitment of nonreceptor proteins into the receptor complex upon intact antibody binding might also contribute to the observed RCT values.

Such structural differences are shown directly by TPA studies on this system (Pecht et al., 1991). H10 mAbs at 5°C show a TPA RCT of 80 μs as compared with 199 μs for the corresponding Fab fragments, this in spite of the expectation of 100% dimer formation. Similarly F4 and J17 mAbs exhibit in TPA no rotational relaxation at 5°C on the timescale of the experiment although the corresponding Fab fragments are rotationally mobile (see above). We conclude that depending on the mAb clone, temperature, etc., various rotational correlation times can be observed for particular receptor-containing species.

The high precision of TPA data has permitted a two-exponential analysis of the rotation of IgE bound to $Fc_\epsilon RI$ (Pecht et al., 1991). Rotational correlation times of 30 and 186 μs with fractional amplitudes of 0.45 and 0.55 were observed. These same data, fitted to a single exponential model, would yield the harmonic mean of the above RCTs or 82 μs. A uniaxially-rotating object like a membrane protein exhibits two RCTs of 1/D and 1/4D where D is the rotational diffusion constant of the object about the rotation axis (Cherry, 1978). The amplitudes of these two components depend upon the orientation of the probe emission and excitation dipoles to each other and to the rotation axis (Jovin and Vaz, 1989). If the object bears randomly-oriented chromophores, the fractional amplitudes of the anisotropy decays corresponding to these RCTs are equal at a value of 0.40 and a limiting anisotropy of fractional amplitude 0.20 is also expected (Rigler and Ehrenberg, 1973). ErITC-IgE seems to be such a ligand and so, for isolated $Fc_\epsilon RI$, we might take 1/D and 1/4D to as be approximately 160 μs and 40 μs, respectively, at 4°C. If receptor dimers were present, rotational correlation times up to 320 μs become possible. Suppose now that $Fc_\epsilon RI$ bind a

ligand labeled at a unique site with a chromophore having a unique orientation. The receptors could now exhibit any RCT within the above ranges. Moreover, rising or falling anisotropies could be observed as well as a variable limiting anisotropy, all according to the probe chromophore orientation. This observation broadly rationalizes all values observed in TPA measurements of $Fc_\epsilon RI$ binding intact anti-receptors antibodies on their Fab fragments. A major cause of changes in RCTs and anisotropy values observed by TPA upon temperature change or upon comparison of monovalent ligand with a bivalent one would be expected to be conformational changes in receptor-ligand structures leading to changes in chromophore orientation. The comparative uniformity of RCTs and initial and final anisotropies observed by PFD for receptors binding eosin-conjugates of these immunochemicals might then reflect more nearly random labeling of the various ligands with EITC. In such a case reorientation of receptor ligands is without effect on rotational parameters (Rigler and Ehrenberg, 1973).

From Table 2, it is clear that receptor RCT decreases with increased temperature for monomeric receptors as well as for receptors binding intact mAbs. The rotational correlation time of monomeric $FC_\epsilon RI$ decreases with temperature from 78–82 μs at 4°C to 60–57 μs at 15°C. Zidovetzki and co-workers reported an average RCT value for receptor monomer that dropped from 65 μs at 5.5°C to 50 μs at 13.8°C (Zidovetzki et al., 1986). The rotational correlation time of receptors binding the intact F4 mAb decreases from 154 ± 7 μs to 124 ± 5 μs when temperature is changed from 15°C to 27°C. The small activation energies of ~5 kcal/mol which these data imply are consistent with unrestricted protein rotation in a membrane lipid environment and appear, as they should, to be grossly independent of the protein size. Thus, unlike other membrane receptors such as epidermal growth factor receptors (Zidovetzki et al., 1985) or luteinizing hormone receptors on luteal cells (Roess et al., 1987), $Fc_\epsilon RI$ do not seem to undergo thermotropic association with themselves or with other membrane components.

We observed, for highly aggregated $Fc_\epsilon RI$, initial anisotropy values of about 0.08, approximately threefold less than the value of 0.24 expected from eosin photophysics (Garland and Moore, 1979). We attribute this difference to rapid motions occurring in the submicrosecond timescale. These rapid motions might include rotation of bound fluorophores, looseness of mAb binding to the $Fc_\epsilon RI$, and perhaps also segmental motion of the cell-bound immunoglobulins in the aqueous external environment. Thus, we conclude that rapid motion of the fluorophores and perhaps segmental flexibility of the antibodies account for depolarization of initial anisotropy to a value approximately 3-fold lower than that expected.

Further, the initial anisotropy values for receptors not highly cross-linked, i.e., binding intact mAbs, their Fab fragments, or IgE, are approximately half those of the aggregated receptors (i.e., 0.04 vs. 0.08). We deduce that, besides the rapid fluorophore motions just discussed, some degree of wobbling of proteins exists about the membrane normal on a timescale too fast for us to observe. We suggest that it is not observed in larger aggregates because of the rigidity of these large structures. This "wobble-in-cone" is analogous to that phenomenon described by Jähnig (1979) for lipids. Thus, rapid fluorophore motions appear to account for depolarization of about two-thirds of the depletion anisotropy initially produced while wobble of membrane proteins removes an additional one-sixth of this initial anisotropy. How much of this wobble can be assigned to the $Fc_\epsilon RI$ and how much to the mAb, Fab, or IgE probe cannot presently be determined. This leaves about one-sixth of the anisotropy theoretically expected, or ~0.040, to decay with rotational relaxation of the protein as a whole.

Finally, the finite limiting anisotropy values we and others (see, for example, Damjanovich et al., 1983; Naqvi et al., 1973) observe in studies of membrane protein rotation are of considerable interest. Kinosita (Kinosita et al., 1977, Kawato and Kinosita, 1981) and Lipari (Lipari and Szabo, 1980) interpret such values in terms of orientational constraints on protein rotation. However we should point out that finite limiting anisotropies may simply demonstrate that membrane proteins cannot rotate freely over two angular variables. If rotational diffusion over two angular variables is possible, the limiting anisotropy should decay to zero. Theories of uniaxial rotation (Rigler and Ehrenberg, 1973) predict that the limiting anisotropy values should be about one-fifth the initial anisotropies. Limiting anisotropy values of this magnitude were in fact observed. Because this value is derived assuming that rotational diffusion is restricted only by dimensional constraints, we are lead to believe that other barriers to rotational diffusion of integral membrane proteins are of limited significance.

This work was supported in part by the National Institutes of Health grants AI21873, and CA46159 (B. George Barisas) and by the National Institutes of Health Biomedical Research Support Grant (B. George Barisas) program. Work done at the Weizmann Institute of Science was generously supported by the Fritz Thyssen Foundation, Germany.

Received for publication 26 February 1991 and in final form 13 September 1991.

REFERENCES

Aroeti, B., T. M. Jovin, and Y. I. Henis. 1990. Rotational mobility of Sendai virus glycoproteins in membranes of fused human erythrocytes and in the envelopes of cell-bound virions. *Biochemistry.* 29:9119–9125.

Austin, R. H., S. S. Chan, and T. M. Jovin. 1979. Rotational diffusion of cell surface components by time-resolved phosphorescence anisotropy. *Proc. Natl. Acad. Sci. USA.* 79:5650–5654.

Baird, B., J. Erikson, B. Goldstein, P. Kane, A. K. Menon, D. Robertson, and D. Holowka. 1988. Progress towards understanding the molecular details and consequences of IgE-receptor cross-linking. *In* Theoretical Immunology, Part One. A. S. Perelson, editor. Addison-Wesley Publishing Co., New York. 41–59.

Balakrishnan, K., F. J. Hsu, A. D. Cooper, and H. M. McConnell. 1982. Lipid hapten containing target membranes can trigger specific immunoglobulin E-dependent degranulation of rat basophilic leukemia cells. *J. Biol. Chem.* 257:6427–6433.

Barsumian, E. L., C. Isersky, M. G. Petrino, and R. P. Siraganian. 1981. IgE-induced histamine release from rat basophilic leukemia cell lines: isolation of releasing and non-releasing clones, *Eur. J. Immunol.* 11:317–323.

Bevington, P. R. 1969. Data reduction and error analysis for the physical sciences. McGraw Hill Inc., New York.

Chapman, D., and C. J. Restall. 1979. Rotational and lateral movements in biomembranes: the dynamics of biomembrane components. *Biochem. Soc. Symp.* 46:139–154.

Cherry, R. J. 1978. Measurement of protein rotational diffusion in membrane by flash photolysis. *Methods Enzymol.* 54:47–61.

Corin, A. F., E. Blatt, and T. M. Jovin. 1987. Triplet-state detection of labeled proteins using fluorescence recovery spectroscopy. *Biochemistry.* 26:2207–2217.

Damjanovich, D., L. Tron, J. Szollosi, R. Zidovetzki, W. L. C. Vaz, F. Regatairo, D. J. Ardnt-Jovin, and T. Jovin. 1983. Distribution and mobility of murine histocompatability H-2K antigen in the cytoplasmic membrane. *Proc. Natl. Acad. Sci. USA.* 80:5985–5989.

Erikson, J., P. Kane, B. Goldstein, and D. Holowka. 1986. Cross-linking of IgE-receptor complexes at cell surface: a fluorescence method for studying the binding of monovalent and bivalent haptens to IgE. *Molec. Immunol.* 72:769–781.

Fewtrell, C., and H. Metzger. 1980. Larger oligomers are more effective than dimers in stimulating rat basophilic leukemia cells. *J. Immunol.* 125:701–710.

Garland, P. B., and P. Johnson. 1985. Rotational diffusion of membranes and proteins. *In* The Enzymes of Biological Membranes. A. N. Martonosi, editor. Plenum Publishing Corp., New York. Vol. 1, chapt. 13.

Garland, P., and C. Moore. 1979. Phosphorescence of protein bound eosin and erythrosin. A possible probe of slow rotational mobility. *Biochem. J.* 183:561–572.

Jähnig, F. 1979. Structural order of lipids and proteins in membrane: evaluation of fluorescence anisotropy data. *Proc. Natl. Acad. Sci. USA.* 76:6361–6365.

Johnson, P. and P. G. Garland. 1982. Fluorescent triplet probes for measuring the rotational diffusion of membrane proteins. *Biochem. J.* 203:313–321.

Jovin, T. M. 1986. Rotational diffusion on cell surfaces: contrasting effect of temperature on epidermal growth factor and Fc (immunoglobulin E) receptors. *Biochem. Soc. Trans.* 14:817–818.

Jovin, T. M., and D. J. Arndt-Jovin. 1989. Luminescence digital imaging microscopy. *Annu. Rev. Biophys. Biophys. Chem.* 18:271–308.

Jovin, T. M., and W. L. Vaz. 1989. Rotational and translational diffusion in membranes measured by fluorescence and phosphorescence methods. *Methods Enzymol.* 172:471–513.

Kinosita, K., S. Kawato, and A. Ikegami. 1977. A theory of fluorescence depolarization decay in membrane. *Biophys. J.* 20:289–305.

Kawato, S., and K. Kinosita, 1981. Time dependent absorption anisotropy and rotational diffusion of proteins in membrane. *Biophys. J.* 36:277–296.

Lipari, G., and A. Szabo. 1980. Effect of librational motion on fluorescence depolarization and nuclear magnetic resonance relaxation in macromolecules and membranes. *Biophys. J.* 30:489–506.

Liu, F. T., J. W. Bohn, E. L. Ferry, H. Yamamoto, C. A. Molinaro, L. A. Sherman, N. R. Klinman, and D. H. Katz. 1980. Monoclonal DNP-specific murine IgE antibody: preparation, isolation, and characterization. *J. Immunol.* 124:2728–2737.

Jovin, T. M., M. Bartholdi, W. L. Vaz, and R. H. Austin. 1981. Rotational diffusion of biological macromolecules by time-resolved (phosphorescence, fluorescence) anisotropy. *Ann. N.Y. Acad. Sci.* 366:176–195.

Johnson, P., and P. Garland. 1981. Depolarization of fluorescence depletion. *FEBS (Fed. Eur. Biochem. Soc.) Lett.* 132:252–256.

Matayoshi, E. D., Sawyer, W. H., and Jovin, T. M. (1991). Rotational diffusion of band 3 in erythrocyte membranes. 2. Binding of cytoplasmic enzymes. *Biochemistry.* 30:3538–3543.

Matayoshi, E. D., T. M. Jovin. 1991. Rotational diffusion of band 3 in erythrocyte membranes. 1. Comparison of ghosts and intact cells. *Biochemistry.* 30:3527–3538.

McCloskey, M. A., Z. Y. Liu, and M. M. Poo. 1984. Lateral electromigration and diffusion of Fc_ϵ receptors on rat basophilic leukemia cells: effects of IgE binding. *J. Cell Biol.* 99:778–787.

Naqvi, K. R., R. J. Gonzales, R. J. Cherry, and D. Chapman. 1973. Spectroscopic technique for studying rotation in membrane. *Nature (Lond.).* 245:249–251.

Niswender, G. D., R. H. Schwall, T. A. Fitz, C. E. Farin, and H. R. Sawyer. 1985. Regulation of luteal function in domestic ruminants: new concepts. Rec. Prog. Hormone Res. 41:101–151.

Ortega, E., R. Schweitzer-Stenner, and I. Pecht. 1988. Possible orientational constraints determine secretory signals induced by aggregation of IgE receptors on most cells. *EMBO Eur. Mol. Biol. Organ. J.* 7:4101–4109.

Ortega, E., R. Schweitzer-Stenner, and I. Pecht. 1989. Possible configuration constraints determine the efficiency of transmembrane signals caused by receptor aggregation: the mast cell case. *Biophys. J.* 55:500*a*. (Abstr.)

Pecht, I., E. Ortega, and T. M. Jovin. 1991. Rotational dynamics of the Fc_ϵ receptor on mast cells monitored by specific monoclonal antibodies. *Biochemistry.* 30:3450–3458.

Rigler, R., and M. Ehrenberg. 1973. Molecular interactions and structure as analyzed by fluorescence relaxation spectroscopy. *Q. Rev. Biophys.* 6:139–199.

Robertson, D., D. Dembo, and B. Baird. 1986. Cross-linking of immunoglobulin E-receptor complexes induces their interaction with the cytoskeleton of rat basophilic leukemia cells. *J. Immunol.* 136:4565–4572.

Roess, D. R., G. Niswender, T. Jovin, and B. G. Barisas. 1987. Rotational diffusion of luteal cell luteal hormone receptor studied

by time-resolved phosphorescence anisotropy. *Biophys. J.* 51:419*a*. (Abstr.)

Sobotka, A. K., M. Dembo, B. Goldstein, H. Metzger, and L. M. Lichtenstein. 1981. Qualitative characterization of histamine release from human basopils by covalently cross-linked IgE. *J. Immunol.* 127:2285–2291.

Saffman, P. G., and G. Delbrück. 1975. Brownian motion in biological membrane. *Proc. Natl. Acad. Sci. USA.* 73:3111–3113.

Schlessinger, J., W. W. Webb, E. L. Elson, and H. Metzger. 1976. Lateral motion and valence of Fc receptor on rat peritoneal mast cell. *Nature (Lond.)* 264:550–552.

Segal, D. M., J. D. Tourog, and H. Metzger. 1977. Dimeric IgE serves as a unit signal for cell degranulation. *Proc. Natl. Acad. Sci. USA.* 74:2993–2997.

Yoshida, T. M., and B. G. Barisas. 1986. Protein rotational motion in solution measured by polarized fluorescence depletion. *Biophys. J.* 50:41–53.

Zidovetzki, R., Y. Yarden, J. D. Schlessinger, and T. M. Jovin. 1985. Rotational diffusion of epidermal growth factor complexed to cell surface receptors reflect rapid microaggregation and endocytosis of occupied receptors. *Proc. Natl. Acad. Sci. USA.* 8:1337–1341.

Zidovetzki R., M. Bartholdi, D. Ardnt-Jovin, and T. M. Jovin. 1986. Rotational dynamics of the FcR for immunoglobulin E on histamine releasing RBL cells. *Biochemistry.* 25:4397–4401.